Vibrations and acoustic noise reduction in A.C. electrical drives. Use of analytical and experimental modal techniques

A. Hubert, G. Friedrich
Laboratoire d'Électromécanique de Compiègne (L.E.C.)
Université de Technologie de Compiègne
Centre de recherche de Royalieu BP 20 529
60205 Compiègne Cedex
France
e-mail: guy.friedrich@utc.fr

Abstract

Electrical machines are nowadays always supplied by power converters to improve speed and torque control capabilities. These converters use a chopping technique to supply A.C. machines with D.C. sources: these converters apply a succession of pulse width modulation where only the fundamental component drives the motor. These techniques permit a very good efficiency but lead to high frequencies components in voltage spectrum. These harmonics lead to an increase of noise especially when they coincide with a mechanical amplification – resonance. This paper treats a study of stator vibrational behaviour and the strategy to avoid excessive noise emission. Further experiments conducted on induction machines are made to validate the proposed models.

1 Introduction

Electrical machines are nowadays always supplied by power converters to improve speed and torque control capabilities. These converters use a chopping technique to supply A.C. machines with D.C. sources: these converters apply a succession of pulse width modulation where only the fundamental component drives the motor. These techniques permit a very good efficiency but lead to high frequencies components in voltage spectrum. Due to the inductive behavior of the machine, these components are not perturbating for the electro-mechanical behaviour (speed and torque) but increase significantly the vibrations of the machine and the noise when the chopping frequency is in the audible range.

Our laboratory has developed a modelisation that permits to express the surface forces that are due to the converter as a superposition of revolving fields with different waveforms and velocity in the airgap of the machine. These modelisation use Fourier Transform in two dimensions (space and time) and the forces obtained are the source of excitation due to the converter. They lead to an increase of noise and vibrations.

The purpose of this paper is to explain how use the characteristics of this force to determine the mechanical behaviour of the machine and to estimate the noise that are radiated. In this way, we develop a modelisation using HAMILTON principle based on the mechanical behaviour of rings. After the obtaining of the motion equations, we study the eigenvalues problem (mode shapes and natural frequencies) and the forced response of the structure when excited by electromagnetic forces. This permits to extract rules to reduce noise and vibrations.

Finally these theoretical results are confirmed by experimental measures done on an 1kW induction motor supply by a power converter. The force density can be easily modified by changing the control strategy of the power converter. That permits a reduction of more than 16 dB of pressure level between a bad and a good tuning of the converter.

2 Short review of noise and vibrations reduction in A.C. electrical drives

Noise and vibrations of electrical drives are not a recent subject of studies. These problems are well doc-

umented in the literature [1] [2] but the fact of supplying a machine with a P.W.M. power converter yields new problems. The purpose of this paper is *not* to treat general noise of vibration in electrical drives but only to focus on the noise that is directly correlated with the use of a power converter. Therefore, the other sources are not taken into account in this paper.

2.1 Use of control techniques

One of the most used techniques to avoid noise due to the power converter is to use components that are switched above audible frequencies. That reduces drastically the perturbating due to the converter. This method, although significantly efficient, can not always be used because high switching are not always possible in high power drive and often leads to an increased lost in power components and therefore reduce the efficiency and the life of the electronic components.

2.2 Determination of the force due to the power converter

To predict the mechanical behaviour of the machine, we first have to determine the electromagnetic forces applied to the structure. The forces are deduced by an electromechanical energy conversion analysis. In fact, the vibrations are principally due to the magnetic fields produced in the airgap of the machine. These fields create a radial force density applied in the inner area of the stator. There is many means to compute these forces – numerical and analytical methods – and our laboratory has developed a modelisation that is well adapt for the coupling to a vibrational modelisation [3] [4]. These models permit to express the surface forces that are due to the converter as a superposition of revolving fields with different waveforms and velocity. These modelisation use Fourier Transform in two dimensions (space and time) and finally, we obtain a radial force density expressed as:

$$f(t,\theta) = \sum_{n=-\infty}^{n=+\infty} \sum_{m=-\infty}^{m=+\infty} \hat{f}_{n\,m} \cdot e^{jn\omega t} \cdot e^{jm\theta} \qquad (1)$$

Where f is the force density applied to the inner surface of the stator, t the temporal variable and θ the angular position. The field f is the source of excitation that is due to the converter and that leads to an increase of the noise and vibrations.

Contrary to the common mind, this modelisation is not linear because the forces applied on the structure result of the MAXWELL stress tensor – MAXWELL force density – that is a quadratic form of the magnetic field. Therefore the frequencies of the forces are *not* the frequencies present in the current and voltage.

3 Theoretical behaviour of the machine

With the use of the electromechanical modelisation developped previously, we can express the radial forces as a superposition of revolving fields that are applied to the inner area of the stator. Generated vibrations of electrical drives can significantly be reduced if the forces can not excite mechanical resonance of the stator. Therefore a precise determination of frequencies and modes shapes are necessary. With the use of a vibration behaviour models, a machine designer will be able to optimize his machine and converter to reduce efficiently noise and vibrations. A well adapted method in this way, is the modal method.

3.1 Short review on the vibrational behaviour of induction electrical motor

For noise reduction in mechanical systems, it is essential to avoid coincidence between excitation and natural behaviour (frequencies *and* mode shapes). In a first step, we will analyse the eigenvalues and eigenvectors problem and in a second step, we will study the forced behaviour. For noise due to the electromagnetic source, it is well known that the most radiated sources are the outer stator areas. A lots of papers exist on numerical determination of stator natural behaviour and we can notice that in all these studies, *in the plane of a sheet*, low frequencies modes shapes are very closed to sinusoidal shapes. For the m rank, with s ($\theta = \frac{s}{R}$) the circumferential length and R the mean radius of stator, we generally have the mode shape U_m as:

$$U_m(s) \approx A_m \cdot \sin(\frac{m \cdot s}{R}) \qquad (2)$$

In stator vibrational behaviour, the contribution of the teeth to the potential energy – elastic strain – is usually negligible whereas it is *not* for kinetic energy [5]. We therefore can include this contribution by changing the mass density of magnetic materials and consider the stator as an *equivalent ring* [6]. The natural frequency of a stator, *in the plane of a sheet* can

therefore be approximated by natural behaviour of an equivalent ring. Our model will follow this hypothesis.

For $m = 0$, we are generally speaking of a pure extensional mode because the strain is principally due to an extension rather than a bending. For $m = 1$, *in the plane of a sheet*, it is a so-called rigid body motion because there is motion without strain and finally for $m \geq 2$ we speak about bending modes (Figure 1).

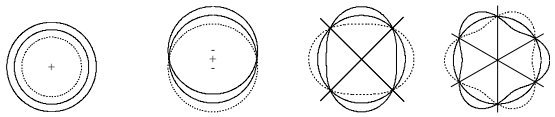

$m = 0$ $m = 1$ $m = 2$ $m = 3$

Figure 1: modal motions for low frequencies, in the plane of a sheet

For the development of our model, we will consider the equivalent ring of radius R and cross section A as described in the Figure 2. We modify the mass density ρ to take into account the teeth mass addition. u and v are radial and tangential displacement of the *mean line*. We assume that the beam can be modelized as a thin beam (EULER - BERNOULLI) [7].

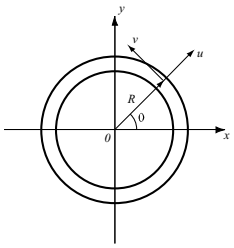

Figure 2: definition of the thin ring

To obtain the motion equations, we will use the HAMILTON theorem that leads to a variation formulation of the problem. Firstly by cancelling the forces, we will express the natural behaviour and secondly, with the electromagnetic forces, we will consider the forced motions.

3.2 Determination of motion equations

We have noticed previously that the $m = 0$ mode can be considerated as a pure extension mode when the others can be considerated as bending modes[1]. We will therefore study these two cases separately with the use of HAMILTON and variational principle applied to a continuum body.

3.2.1 Pure extension motions

For $m = 0$ mode, we have a displacement that is purely radial (only $u \neq 0$) but a strain that is purely tangential (only $\epsilon_{\theta\theta} \neq 0$). The momentum is $p = \rho \cdot A \cdot \frac{\partial u}{\partial t}$ and the velocity $\frac{\partial u}{\partial t}$, that leads to the following kinetic energy:

$$\mathcal{T} = \frac{1}{2} \cdot \int_0^l \vec{p} \cdot (\frac{\partial \vec{u}}{\partial t})\, ds = \frac{1}{2} \cdot \int_0^l \rho \cdot A \Big(\frac{\partial u}{\partial t}\Big)^2 ds \quad (3)$$

In the case of a pure extension, elongation per unit for the ring in circonferential direction s equal $\varepsilon_{\theta\theta} = \frac{\partial v}{\partial s}$. Potential energy of deformation is, in this case, the deformation energy of a simple extension. Normal force N equals normal constraint $\sigma_{\theta\theta}$ multiplied by the cross section A ($N = A \cdot \sigma_{\theta\theta}$). If we consider the deformation as an elastic deformation , we can use the YOUNG formula that relies the constraint $\sigma_{\theta\theta}$ and the deformation $\epsilon_{\theta\theta}$ with the YOUNG modulus E ($\sigma_{\theta\theta} = E \cdot \varepsilon_{\theta\theta} = E \cdot \frac{\partial v}{\partial x}$). Therefore, we obtain the following potential energy:

$$\mathcal{V} = \frac{1}{2} \cdot \int_0^l \vec{F_x} \cdot (\frac{\partial \vec{u}}{\partial x})\, ds = \frac{1}{2} \cdot \int_0^l E \cdot A \Big(\frac{\partial v}{\partial s}\Big)^2 ds \quad (4)$$

HAMILTON theorem specifies that if we consider an external force f_i and if $\mathcal{L} = \mathcal{T} - \mathcal{V}$ is defined as the LAGRANGIAN of the system, therefore the following variational formulation must be zero for *any admissible variation* δx_i (*virtual displacement*) between the two time t_1 and t_2 [8]:

$$\int_{t_1}^{t_2} (\delta\mathcal{L} + \sum_i f_i \cdot \delta x_i)\, dt = 0 \quad (5)$$

If u is the radial displacement of any point of the ring, therefore the strain per unit in circonferential direction (extensional strain : $\epsilon_{\theta\theta} = \frac{\partial v}{\partial s}$) equals $\frac{u}{R}$. An admissible displacement for external efforts is δu. By using HAMILTON principle, this leads to:

$$\int_{t_1}^{t_2} \delta\Big(\int_0^l \frac{1}{2} \cdot \rho \cdot A \Big(\frac{\partial u}{\partial t}\Big)^2 - \frac{1}{2} \cdot E \cdot A \Big(\frac{u}{R}\Big)^2 ds \Big) + \int_0^l (f \cdot \delta u)\, ds\, dt = 0 \quad (6)$$

This equation can be modified by the use of variational calculus – integration by parts – and finally, we

[1] We will see that rigid body motion – $m = 1$ – can be, in a first step, included in the bending case

obtain:

$$\int_{t_1}^{t_2}\int_0^l -\rho\cdot A\frac{\partial^2 u}{\partial t^2}\cdot\delta u - \frac{E\cdot A}{R^2}u\cdot\delta u + f\cdot\delta u\,ds\,dt = 0 \tag{7}$$

We can factorized the term δu. This relation must hold for any δu, then we deduce the motion equation:

$$-\rho\cdot A\frac{\partial^2 u}{\partial t^2} - \frac{E\cdot A}{R^2}u + f = 0 \tag{8}$$

3.2.2 Bending motions

In the case of pure bending motion, tangential displacement is not zero ($v \neq 0$), this leads to the following kinetic energy:

$$\mathcal{T} = \frac{1}{2}\cdot\int_0^l \rho\cdot A\cdot\Big(\Big(\frac{\partial u}{\partial t}\Big)^2 + \Big(\frac{\partial v}{\partial t}\Big)^2\Big)\,ds \tag{9}$$

For a bending motion, potential energy equal bending moment multiplied by the curvature variation. We consider the ring as sufficiently thin to use EULER-BERNOULLI hypothesis:

- We can neglect shear deformation
- We can neglect rotation inertia of a cross section

For a curved beam, we have a curvature variation that is [9]:

$$\frac{1}{R+\Delta R} - \frac{1}{R} = \frac{\partial^2 u}{\partial s^2} + \frac{u}{R^2} \tag{10}$$

We can also consider that in a bending motion, the elongation of neutral fiber can be neglected [10]:

$$\epsilon_{\theta\theta} = \frac{u}{R} + \frac{\partial v}{\partial s} \approx 0 \tag{11}$$

Then, we have $u = -R\cdot\frac{\partial v}{\partial s}$. In bending theory, the bending moment equal curvature variation multiplied by the factor $E.{I_{Gz}}^2$. We obtain the following potential energy:

$$\mathcal{V} = \frac{1}{2}\cdot\int_0^l E\cdot I_{Gz}\Big(\frac{\partial^2 u}{\partial s^2} + \frac{u}{R^2}\Big)^2\,ds \tag{12}$$

The electromagnetic effort are considered as radial, the work resulting of these efforts will be in the direction of a radial virtual displacement δu. We can therefore apply the HAMILTON theorem:

$$\begin{aligned}&\int_{t_1}^{t_2}(\delta\int_0^l \frac{1}{2}\cdot\rho\cdot A\Big(\Big(\frac{\partial u}{\partial t}\Big)^2 + \Big(\frac{\partial v}{\partial t}\Big)^2\Big)\\ &-\frac{1}{2}\cdot E\cdot I_{Gz}\Big(\frac{\partial^2 u}{\partial s^2} + \frac{u}{R^2}\Big)^2\,ds\\ &+\int_0^l f\cdot\delta u)\,dt = 0\end{aligned} \tag{13}$$

[2] this coefficient is know as the bending stiffness or flexural rigidity and $I_{Gz} = \int_A y^2\,dA$ as the area moment of inertia

As previously, we use variational calculus – integrations by part according to t and s. We must notice that the structure – a ring – is periodic therefore some terms vanish. After some manipulations, we obtain:

$$\begin{aligned}&\int_{t_1}^{t_2}\int_0^l \Big(-\rho\cdot A\Big(\frac{\partial^2}{\partial t^2}(-R^2\frac{\partial^2 v}{\partial s^2} + v)\Big)\\ &-E\cdot I_{Gz}\Big(-R^2\cdot\frac{\partial^6 v}{\partial s^6} - 2\cdot\frac{\partial^4 v}{\partial s^4}\\ &-\frac{1}{R^2}\cdot\frac{\partial^2 v}{\partial s^2}\Big) + R\cdot\frac{\partial f}{\partial s}\Big)\cdot\delta v\,ds\,dt = 0\end{aligned} \tag{14}$$

This equation must hold for any admissible displacement δv, we therefore obtain the motion equation:

$$\begin{aligned}&-\rho\cdot A\Big(\frac{\partial^2}{\partial t^2}(-R^2\frac{\partial^2 v}{\partial s^2} + v)\Big)\\ &-E\cdot I_{Gz}\Big(-R^2\cdot\frac{\partial^6 v}{\partial s^6} - 2\cdot\frac{\partial^4 v}{\partial s^4} - \frac{1}{R^2}\cdot\frac{\partial^2 v}{\partial s^2}\Big)\\ &+R\cdot\frac{\partial f}{\partial s} = 0\end{aligned} \tag{15}$$

3.3 Eigenvalue problem

After the obtaining of the motion equations, we will study the natural behaviour of the machine. Yet, we are cancelling the external forces f and we obtain an eigenvalue problem. As previously, we study in a first step, extension motion and in a second, bending motions.

3.3.1 Pure extension motions

We start with the equation (8) by considering f as zero. We are looking for the separate variables solution $u(t,s) = \phi_0(t)\cdot U_0(s)$ this leads to:

$$-\rho\cdot A\cdot\ddot{\phi}_0(t)\cdot U_0(s) - \frac{E\cdot A}{R^2}\cdot\phi_0(t)\cdot U_0(s) = 0 \tag{16}$$

that can be rewritten:

$$-\frac{\ddot{\phi}_0(t)}{\phi_0(t)} = \frac{E\cdot A}{\rho\cdot A\cdot R^2} = p_0^2 \tag{17}$$

There is only one solution to this equation – one frequency p_0 – because the others are solutions of bending modes. We obtain for this mode, an U_0 eigenmode that does not depend on s ($U_0 = constant = \hat{A}_0$). In *elastodynamic*, we usually normalize this mode according to the mass:

$$\int_0^l U_0\cdot\rho\cdot A\cdot U_0\,ds = 1 \tag{18}$$

Therefore, we have $\hat{A}_0 = \frac{1}{\sqrt{2\cdot\pi\cdot R\cdot\rho\cdot A}}$.

3.3.2 Bending motions

For this mode, we use the equation (15), without f. There are yet many bending modes, the separate variables solution is writing as $v(t,s) = \sum_i \phi_i(t) \cdot V_i(s)$. With $V_i^{(k)} = \frac{\partial^k V_i}{\partial s^k}$, we obtain:

$$\begin{aligned}&\sum_i -\rho \cdot A\Big(\ddot{\phi}_i(t) \cdot V_i(s) - R^2 \cdot \ddot{\phi}_i(t) \cdot V_i^{(2)}\Big)\\&+ E \cdot I_{Gz}\Big(R^2 \cdot \phi_i(t) \cdot V_i^{(6)} + 2 \cdot \phi_i(t) \cdot V_i^{(4)}\\&+ \frac{1}{R^2} \cdot \phi_i(t) \cdot V_i^{(2)}\Big) = 0\end{aligned} \tag{19}$$

And for $i = m$:

$$\begin{aligned}&-\frac{\ddot{\phi}_m(t)}{\phi_m(t)} =\\&-\frac{E \cdot I_{Gz}}{\rho \cdot A} \cdot \frac{R^2 \cdot V_m^{(6)} + 2 \cdot V_m^{(4)} + \frac{1}{R^2} \cdot V_m^{(2)}}{V_m(s) - R^2 \cdot V_m^{(2)}}\end{aligned} \tag{20}$$

The variables t et s are independent, therefore right and link members must hold simultaneously. With $-\frac{\ddot{\phi}_m(t)}{\phi_m(t)} = p_m^2$, we obtain the eigenvalue problem:

$$\begin{aligned}&-\frac{E \cdot I_{Gz}}{\rho \cdot A} \cdot \frac{R^2 \cdot V_m^{(6)} + 2 \cdot V_m^{(4)} + \frac{1}{R^2} \cdot V_m^{(2)}}{V_m(s) - R^2 \cdot V_m^{(2)}}\\&= p_m^2\end{aligned} \tag{21}$$

The solutions are complex exponential functions, but the continuity boundary condition ($V_m(s = 0) = V_m(s = l)$) restricts the solution to harmonic functions:

$$V_m = \hat{A}_m \cdot e^{j \cdot \frac{m \cdot s}{R}} \tag{22}$$

For m, we have:

$$\frac{1}{R^4} \cdot \frac{m^2 \cdot (m^2-1)^2}{(1+m^2)} = p_m^2 \cdot \frac{\rho \cdot A}{E \cdot I_{Gz}} \tag{23}$$

This leads to these eigenvalues and vectors according to the literature [6]:

$$\begin{aligned}&p_{m^2} = \frac{E \cdot I_{Gz}}{\rho \cdot A \cdot R^4} \cdot \frac{m^2 \cdot (m^2-1)^2}{(1+m^2)}\\&V_m(s) = \hat{A}_m \cdot e^{j \cdot \frac{m \cdot s}{R}}\end{aligned} \tag{24}$$

We normalize the eigenvector according to the mass and obtain $\hat{A}_m = \hat{A}_0$.

3.4 Forced response of the structure

For the study of forced motions, we use the dynamic equations that are projected on each mode shape.

3.4.1 Pure extension motion

We project the extension motion equation on U_0 mode:

$$\int_0^l (-\rho \cdot A \cdot \frac{\partial^2 u}{\partial t^2} - \frac{E \cdot A}{R^2} \cdot u + f) \cdot U_0 \, ds = 0 \tag{25}$$

We express $u(t,s)$ on modal basis, this means with $-\infty \leq i \leq +\infty$, 0 included, on the form $u(t,s) = \sum_i \phi_i(t) \cdot U_i(s)$. We have seen that $U_{i=0}$ is a constant and the others $U_{i\neq 0}$ are complex exponentials. The projection on U_0 mode can be different from zero only for this 0 mode ($\int_0^l U_0 \cdot U_{i\neq 0} \, ds = 0$), this leads to:

$$\begin{aligned}&\int_0^l -\rho \cdot A \cdot \ddot{\phi}_0(t) \cdot U_0(s) \cdot U_0(s)\\&- \frac{E \cdot A}{R^2 \cdot \rho \cdot A} \cdot \rho \cdot A \cdot \phi_0(t) \cdot U_0(s) \cdot U_0(s)\\&+ f \cdot U_0(s) \, ds = 0\end{aligned} \tag{26}$$

With the normalization ($\int_0^l U_0 \cdot \rho \cdot A \cdot U_0 \, ds = 1$) and the definition of the eigenfrequency ($p_0^2 = \frac{E \cdot A}{R^2 \cdot \rho \cdot A}$), we have:

$$\ddot{\phi}_0(t) + p_0^2 \cdot \phi_0(t) = \int_0^l f \cdot U_0 \, ds = 0 \tag{27}$$

This equation is known as modal equation on 0 mode and $F_0 = \int_0^l f \cdot U_0 \, ds$ is a *modal force* or *generalized force*.

3.4.2 Bending motions

As previously, we project the dynamic equation (15) on $V_{m\neq 0}$ modes:

$$\begin{aligned}&\int_0^l (-\rho \cdot A\Big(\frac{\partial^2}{\partial t^2}(-R^2 \frac{\partial^2 v}{\partial s^2} + v)\Big)\\&- E \cdot I_{Gz}\Big(-R^2 \cdot \frac{\partial^6 v}{\partial s^6} - 2 \cdot \frac{\partial^4 v}{\partial s^4} - \frac{1}{R^2} \cdot \frac{\partial^2 v}{\partial s^2}\Big)\\&+ R \cdot \frac{\partial f}{\partial s}) \cdot V_m(s) \, ds = 0\end{aligned} \tag{28}$$

We use variation calculus to simplify this equation and we obtain:

$$\begin{aligned}&\int_0^l -\rho \cdot A\Big(\frac{\partial^2}{\partial t^2}\Big(-R^2 \cdot v(t,s) \cdot \frac{\partial^2 V_m(s)}{\partial s^2}\\&+ v(t,s) \cdot V_m(s)\Big)\Big) + E \cdot I_{Gz}\Big(R^2 \cdot v(t,s) \cdot \frac{\partial^6 V_m(s)}{\partial s^6}\\&+ 2 \cdot v(t,s) \cdot \frac{\partial^4 V_m(s)}{\partial s^4} + \frac{1}{R^2} \cdot v(t,s) \cdot \frac{\partial^2 V_m(s)}{\partial s^2}\Big)\\&- \Big(R \cdot f(t,s) \cdot \frac{\partial V_m(s)}{\partial s}\Big) \, ds = 0\end{aligned} \tag{29}$$

We have seen that $V_m(s) = \hat{A}_m \cdot e^{j \cdot \frac{m \cdot s}{R}}$, $\frac{\partial^2 V_m(s)}{\partial s^2} = -\frac{m^2}{R^2} \cdot V_m(s)$ and the eigenproblem gives:

$$\begin{aligned} &-(R^2 \cdot V_m^{(6)} + 2 \cdot V_m^{(4)} + \frac{1}{R^2} \cdot V_m^{(2)}) \\ &= (p_m^2 \cdot \frac{\rho \cdot A}{E \cdot I_{Gz}}) \cdot (V_m - R^2 \cdot V_m^{(2)}) \end{aligned} \tag{30}$$

we replace and obtain:

$$\begin{aligned} &\int_0^l \Big(-\rho \cdot A \Big(\frac{\partial^2}{\partial t^2} (v(t,s) \cdot m^2 \cdot V_m(s) \\ &+ v(t,s) \cdot V_m(s)) \Big) - E \cdot I_{Gz} \Big(p_m^2 \cdot \frac{\rho \cdot A}{E \cdot I_{Gz}} \Big) \\ &\cdot \Big(v(t,s) \cdot V_m(s) + v(t,s) \cdot m^2 \cdot V_m(s) \Big) \\ &- R \cdot f(t,s) \cdot \frac{j \cdot m}{R} \cdot V_m(s) \Big) \, ds = 0 \end{aligned} \tag{31}$$

Yet, we can express v on the modal basis: $\sum_i \phi_i(t) \cdot V_i(s)$ in using these properties (orthogonality between each mode: $\int_0^l V_m \cdot V_{i \neq m} \, ds = 0$ and normalization : $\int_0^l V_m \cdot \rho \cdot A \cdot V_m \, ds = 1$). We obtain these decoupled modal equations:

$$\begin{aligned} &-\ddot{\phi}_m(t) \cdot (1 + m^2) - p_m^2 \cdot \phi_m(t) \cdot (1 + m^2) \\ &- \int_0^l (R \cdot f(t,s) \cdot \frac{j \cdot m}{R} \cdot V_m(s)) \, ds = 0 \end{aligned} \tag{32}$$

With the modal force $F_m = \frac{1}{1+m^2} \cdot \int_0^l (R \cdot f(t,s) \cdot \frac{j \cdot m}{R} \cdot V_m(s)) \, ds$, we obtain the well known equations:

$$\ddot{\phi}_m(t) + p_m^2 \cdot \phi_m(t) = F_m \tag{33}$$

3.5 Application to the electromagnetic forces

We have seen in the first part that the electromagnetic forces can be expressed as a superposition of harmonic revolving fields (with $\theta = \frac{s}{R}$).

$$f(t,s) = \sum_n \sum_m \hat{f}_{n,m} \cdot e^{j \cdot n\omega t} \cdot e^{j \cdot \frac{m \cdot s}{R}} \tag{34}$$

Generalized forces will be the projection of these forces on each mode. We noticed an orthogonality between modes of different ranks, in this case, we have only one term that is different from zero, when the mode and the force have the same m rank. For $m = 0$ (extension), we have:

$$\begin{aligned} F_0(t) &= \int_0^l f(t,s) \cdot U_0 \, ds \\ &= \int_0^l \sum_n \hat{f}_{n,0} \cdot e^{j \cdot n\omega t} \cdot \hat{A}_0 \, ds \\ &= 2\pi \cdot R \cdot \hat{A}_0 \cdot \sum_n \hat{f}_{n,0} \cdot e^{j \cdot n\omega t} \end{aligned} \tag{35}$$

and for $m \neq 0$ (bending) :

$$\begin{aligned} F_m &= \frac{1}{1+m^2} \cdot \int_0^l (R \cdot f(t,s) \cdot \frac{j \cdot m}{R} \cdot V_m(s)) \, ds \\ &= \frac{m}{1+m^2} \cdot 2\pi \cdot R \cdot j \cdot \hat{A}_m \cdot \sum_n \hat{f}_{n,m} \cdot e^{j \cdot n\omega t} \end{aligned} \tag{36}$$

In these two cases, we obtain a second order differential equation. This equation is excited by an harmonic force. The solution of this system is well known, for an $n\omega$ pulsation, this results to:

$$\phi_m(t) = \sum_n \frac{F_{n,m}}{p_m^2 - (n\omega)^2} \cdot e^{j \cdot n\omega t} \tag{37}$$

For the u solution due to the 0 mode, we come back to the initial basis with[3]:

$$\begin{aligned} u(t,s) &= \phi_0(t) \cdot U_0(s) \\ &= \sum_n \frac{2\pi \cdot R \cdot \hat{A}_0 \cdot \hat{A}_0^* \cdot \hat{f}(n,0)}{p_0^2 - (n\omega)^2} \cdot e^{j \cdot n\omega t} \\ &= \sum_n \frac{\hat{f}(n,0)}{(\rho \cdot A) \cdot (p_0^2 - (n\omega)^2)} \cdot e^{j \cdot n\omega t} \end{aligned} \tag{38}$$

For bending modes – $m \neq 0$ –, we obtain for v:

$$\begin{aligned} v(t,s) &= \sum_m \phi_m(t) \cdot V_m \\ &= \sum_n \sum_m \frac{-j \cdot m \cdot \hat{f}(n,m)}{(\rho \cdot A) \cdot (1+m^2) \cdot (p_m^2 - (n\omega)^2)} \\ &\cdot e^{j \cdot n\omega t} \cdot e^{j \cdot \frac{m \cdot s}{R}} \end{aligned} \tag{39}$$

That leads for $u(t,s)$ in using $u(t,s) = -R\frac{\partial v}{\partial s}$:

$$\begin{aligned} u(t,s) = &\sum_n \sum_m \frac{m^2 \cdot \hat{f}(n,m)}{(\rho \cdot A) \cdot (1+m^2) \cdot (p_m^2 - (n\omega)^2)} \\ &\cdot e^{j \cdot n\omega t} \cdot e^{j \cdot \frac{m \cdot s}{R}} \end{aligned} \tag{40}$$

Final solution is the joining of the $m = 0$ solution (extension) and $m \neq 0$ solution (bending). When

[3] with $\hat{A}_0^*$, complex conjugate of $\hat{A}_0$

using the factor K_m defined as:

$$K_m = \begin{cases} 1, & \text{if } m = 0; \\ \frac{m^2}{1+m^2}, & \text{if } m \neq 0. \end{cases} \quad (41)$$

We obtain for radial displacement, with n and m from $-\infty$ to $+\infty$:

$$u(t,s) = \sum_n \sum_m K_m \cdot \frac{\hat{f}(n,m)}{(\rho \cdot A) \cdot (p_m^2 - (n\omega)^2)} \cdot e^{j \cdot n\omega t} \cdot e^{j \cdot \frac{m \cdot s}{R}} \quad (42)$$

In this section, we have proposed a dynamic model for the stator excited by electromagnetic forces. We can express the solution into the form of the equation (42) joining extension and bending motions. We can already notice:

- Only forces with the same spatial rank as a mode shape can be projected on it.
- Modal response is a second order differential equation excited by harmonic forces.
- We have neglected damping, therefore these models hold only for a force with the same space rank far from the natural frequency.
- If there is a frequency coincidence without spatial coincidence, there must be no resonance.
- The $m = 1$ mode was included in bending and we find a zero frequency that is characteristic of rigid body motion. Nowadays we will see that further in 3D motions, this mode will become a longitudinal mode – beam mode – with a non zero frequency.

4 Experimental verifications

4.1 Description of the machine

The machine used for experimental verifications was design in Laboratoire d'Électromécanique de Compiègne (L.E.C.). Therefore the geometric characteristics are perfectly known. It is a 3-phase induction machine supplied by a low voltage (between 9 and 12 V) at a power of 700 W. The machine has $Z_p = 2$ pairs of poles (1500 rpm when supplied by a 50 Hz network). The stator has $Z_s = 27$ slots, 2 layers and the rotor is a $Z_r = 21$ slots squirrel cage rotor (Figure 3). This motor has a diameter of 200 mm and a length of 400 mm.

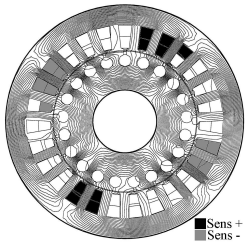

Figure 3: description of the machine

4.2 Natural behaviour

Teeth are not directly taking into account in our model but indirectly by the modified mass density. Modal frequencies are computed with previous formulas and corrected by a factor for bending modes ($K_2 = 1.14$, $K_3 = 1.04$, $K_4 = 1.02$ et $1 \leq K_{\geq 5} \leq 1.015$) extracted from [11] to take into account the third dimension – longitudinal – that influences short shell (and therefore sheets). These values are compared with F.E.A. results, a shock method and a complete modal analysis with an LMS acquisition and processing system. The Finite Element Analysis was realized with I.D.E.A.S software. The computation was done in two dimensions for the stator core without taking into account the winding that usually increases the damping but does not change much the lower modes shapes and frequencies [12]. The boundary conditions were chosen as free. We have measured these frequencies by two different experimental methods: the first was an impact test. The hammer can excite the structure up to 7000 Hz, therefore the measure can be done above. The second method is a more precise modal analysis: it permits a better precision but requires more time and facilities. The excitation was realized by a sinusoidal force at different frequencies with the use of a shaker. The output measures was done at different positions around the structure to extract not only the spectrum but also the modal shape associated with each natural frequency. This experiment was realized up to 10000 Hz therefore the measure can be expressed above. These measures are reported on Figure 4, 5 and 6. These three modes shapes correspond to the three first sinusoidal mode shape computed theoretically for $m = 1$, $m = 2$ and $m = 3$.

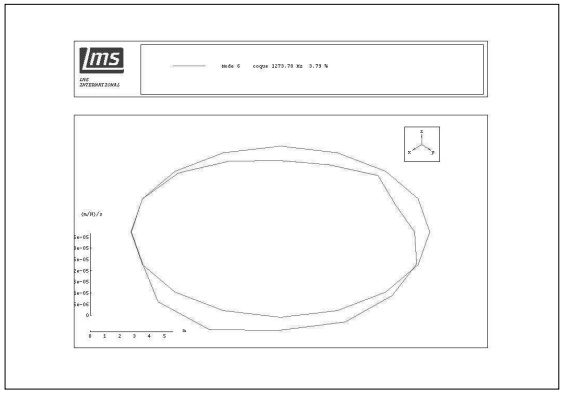

Figure 4: first mode shape: 2 nodes at $f_1 = 1278$ Hz

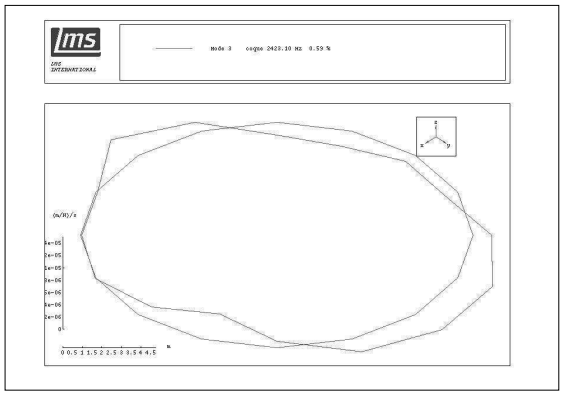

Figure 5: second mode shape: 5 nodes at $f_2 = 2423$ Hz

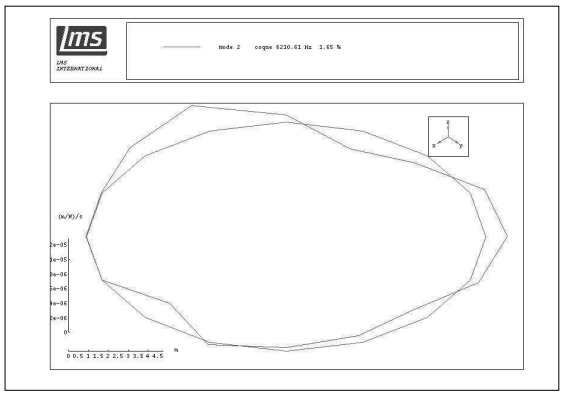

Figure 6: third mode shape: 6 nodes at $f_3 = 6210$ Hz

The first experimental method was done with the machine placed on a low stiffness support and the motor can be considered having free boundaries. The second experiment was done with the motor fixed on its testing bench by the frontface. The results are reported in Table 1 in Hz.

Mode number	Analytical method	Finite Element	Shock method	Modal analysis
0	14859	14656	O. R.	O. R.
1	0	0	1200	1273
2	2478	2364	2400	2423
3	6396	6473	6100	6210
4	12028	11898	11700	O. R.

Table 1: Natural frequencies by 4 different methods (O. R.: Out of Range) in Hz

The results obtained with the analytical method are very close to the results obtained with the other methods. Therefore, this simple method can be used if we employ properly the mass density modification and the coefficients given in the previous section. For example, in this machine, the density of the sheet is 7650 kg/m^3. We have neglected the teeth bending rigidity and having taken into account its mass by modifying the density of the ring. It leads to a new density of 10613 kg/m^3. We have also used the coefficient given before for the frequencies of rank greater than 2. We can notice that when the motor is fixed on its frontface, the natural frequencies are not really different from a free fixation (free boundary conditions). We can also notice that the rigid body motion in a plane of a sheet (in a 2D analysis) is not a rigid body motion in 3D (natural frequency different from zero). In fact, it corresponds to the first bending mode of the stator in the longitudinal dimension (beam mode).

4.3 Forced behaviour

For the verification of the forced behaviour, the machine is supplied by a P.W.M. natural sampling power converter. We can modify f_f the fundamental frequency and f_c the chopping frequency. For this type of converters, the principal harmonic components in the voltage spectrum are at the frequencies f_f, $f_c \pm f_f$, $f_c \pm 2f_f$, $f_c \pm 4f_f$, $2f_c \pm f_f$, $2f_c \pm 4f_f$, $2f_c \pm 5f_f \ldots$ We give an example of this spectrum voltage in Figure 7 for $f_c = 1500$ Hz and $f_f = 50$ Hz in log scale (dB).

To reduce the noise and vibrations of the machine, it is important to compare 2D spectrum of excitation with 2D spectrum of natural frequencies. We have

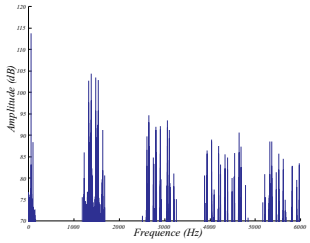

Figure 7: Amplitude of voltage spectrum for a chopping frequency at $f_c = 1500$ Hz and a fundamental frequency at $f_f = 50$ Hz. in log scale (dB)

realized this comparison when the motor is supplied by a natural sampling power converter. The motor is supplied by using different carrier frequencies but always with the same fundamental component (50 Hz, 10 V). In the spectrum of excitations, if we neglect too low amplitude components (more than a hundred times smaller), only the 2 space rank of excitations can approach a mode shape of the stator. This mode shape for the 2 rank has a frequency around 2450 Hz.

With a carrier frequency of nearly 1500 Hz (1428 Hz), we find components with 2 space rank at 1802, 1902, 1952, 2052, 2102 and 2202 Hz. They are spaced of 100 Hz multiples due to the fundamental frequency at 50 Hz. These components correspond to the interaction between 1) the fundamental component $n_1\omega$, 2) the harmonic components around the chopping frequency $n_2\omega$ and 3) the slots harmonics (modulation due to the permeance function). The corresponding force frequency is at the pulsation $n_1\omega + n_2\omega \cdot (1 + \frac{Z_r \cdot (1-\hat{s})}{Z_p})$ with $\hat{s}$ the induction motor slip. The corresponding space ranks is $Z_s - Z_r - 2 \cdot p_0 = 27 - 21 - 2 \cdot 2 = 2$ ([13]) and therefore have the same space rank that the mode shape at 2450 Hz. In this case, these excitations are far enough from the natural frequency therefore the noise and vibrations are relatively low. If we choose another carrier frequency for the power converter, for example 2000 Hz, the new components of $m = 2$ space rank have the frequencies 2374, 2474, 2524, 2624, 2674 and 2774 Hz. We notice, in this case, a component at 2474 Hz that is really close to the natural frequency at 2450 Hz therefore it leads to a strong resonance that increases significantly the noise emitted by the motor as it will be seen later. We can also notice that the frequencies of these excitations are not the frequencies present in the voltage and the current spectrum but differ because of the permeance modulation.

There are different models to express the acoustic pressure versus vibration velocity (see example [1]), we have also developed and used an analytical model of wave radiation in [14] but it is not the purpose of this paper. We will just prove that a non-proper tuning of the converters can become the main noise source in an electrical drive and our method allows rapid diagnostics and a new tuning. The acoustic measures were made in a semi-anechoic room for different positions around the machine. The measurements reported in this article correspond to the principal direction and level of radiation. This direction corresponds to a radial direction in the middle of the stator (the vibration displacement due to the MAXWELL tensor is principally a radial displacement). The measurements reported are pressure levels ($L_p = 10 \cdot \log(\frac{p_{RMS}}{p_0})^2$ with $p_0 = 2 \cdot 10^{-5}$ N.m^{-2}) for components at different frequencies at a distance of one meter, measured with pressure microphones. The acquisition, treatment and signal processing were performed with a PC computer and the help of numerical analysis software. These results are reported on the Table 2 and on the Figure 8 for the spectrum of pressure level at chopping frequency equal 2000 Hz (strong resonance at 2474 Hz).

Chopping frequency (Hz)	Preponderant pressure frequency (Hz)	Pressure level amplitude (dB)
1500	2047	48
2000	2465	59
2500	2030	43

Table 2: Comparison between acoustic pressure level amplitude versus chopping frequency of the power converter

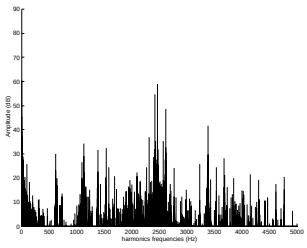

Figure 8: Spectrum of pressure level at chopping frequency equal 2000 Hz

In our experiment, we notice an excitation that appears close to the second resonance ($n = 2$ at frequency equal to 2465 Hz) when the chopping fre-

quency approaches 2000 Hz. This coincidence leads to a strong resonance. If we modify the chopping frequency, we can strongly decrease this resonance and therefore the noise emission. We can decrease the acoustic pressure level by more than 16 dB only by increasing the chopping frequency of 500 Hz. At a chopping frequency equal to 2500 Hz, we obtain 43 dB of pressure level instead of 59 dB at a chopping frequency equal to 2000 Hz because the force frequencies are far from 2465 Hz whereas voltage frequencies are closed (non linearity). We can also notice that a change in the carrier frequency of 100 Hz is enough to already decrease significantly the noise.

5 Conclusion

In this article, we present a short review of the noise in electrical AC drive due to the power converter. We explain how can be expressed the electromagnetic forces. We proposed a model for vibration behaviour that is verified experimentally by modal analysis. We came to the conclusion that only the forces with the same space rank than the mode shape can be projected on it, and then, excite it. If there is a frequential coincidence without spatial coincidence, there is no resonance and therefore no strong additional noise. With these electromagnetic and mechanic models, it is possible to choose the best strategy of the power converter to *place* the annoying forces components far from a resonance with the same space rank and therefore reduce significantly the emitted noise.

Acknowledgements

Many colleagues helped us in various ways but the authors would like to mention particularly R. DIB, J.C. HENRIO and P. WAGSTAFF of the Compiègne University for the help in the realization of modal analysis and P. MACRET for the help in the acoustic measures realized in anechoic room.

References

[1] S.J. YANG. *Low-noise electrical motors*. Clarendon Press, Oxford University Press, 1981.

[2] P.L. TIMAR et al. *Noise and vibrations of electrical machines*. Elsevier, 1989.

[3] A. HUBERT and G. FRIEDRICH. A method for choosing the power converter control strategy to reduce the acoustic noise by taking into account the mechanical structure response. In *E.P.E. 2001*, 2001.

[4] A. HUBERT and G. FRIEDRICH. Influence of power converter on induction motor acoustic noise: interaction between control strategy and mechanical structure. *IEE PROC.-Elec. Power Appl.*, 149(2), March 2002.

[5] J.P. DEN HARTOG. *Mechanical vibrations* 4^{th} *ed.* Dover publications Inc. (Originally published : McGraw-Hill 1956), 1985.

[6] P. VIJAYRAGHAVAN and R. KRISHNAN. Noise in electric machines : a review. *IEEE Trans. on I.A.*, 35(5), Sept./Oct. 1999.

[7] L. MEIROVITCH. *Principles and techniques of vibrations*. Prentice-Hall international Inc., 1997.

[8] S.H. CRANDALL et al. *Dynamics of mechanical and electromechanical systems*. Mc Graw-Hill, 1968.

[9] S.P. TIMOSHENKO. *Résistance des matériaux*. Dunod, 1968.

[10] A.E.H. LOVE. *A treatise on the mathematical theory of elasticity*. Dover publications Inc., 1944.

[11] L. CREMER, M. HECKL, and E.E. UNGAR. *Structure-Borne Sound*. Springer-Verlag, 1988.

[12] S.P. VERMA, K. WILLIAMS, and R.K. SINGAL. Vibration of long and short laminated stator of electrical machines. *Journal of Sound and Vibrations*, 129, 1989.

[13] P.L. ALGER. *Induction Machines : their behavior and uses*. Gordon & Breach Science Publishers, 1970.

[14] A. HUBERT. *Contribution à l'étude des bruits acoustiques générés lors de l'association machines électriques - convertisseurs statiques de puissance. Application à la machine asynchrone*. PhD thesis, Université de Technologie de Compiègne, 2000.